

# RSC Advances



This is an *Accepted Manuscript*, which has been through the Royal Society of Chemistry peer review process and has been accepted for publication.

*Accepted Manuscripts* are published online shortly after acceptance, before technical editing, formatting and proof reading. Using this free service, authors can make their results available to the community, in citable form, before we publish the edited article. This *Accepted Manuscript* will be replaced by the edited, formatted and paginated article as soon as this is available.

You can find more information about *Accepted Manuscripts* in the [Information for Authors](#).

Please note that technical editing may introduce minor changes to the text and/or graphics, which may alter content. The journal's standard [Terms & Conditions](#) and the [Ethical guidelines](#) still apply. In no event shall the Royal Society of Chemistry be held responsible for any errors or omissions in this *Accepted Manuscript* or any consequences arising from the use of any information it contains.

Cite this: DOI: 10.1039/c0xx00000x

www.rsc.org/xxxxxx

ARTICLE TYPE

# Statistic Single-Cell Analysis of Cell Cycle-Dependent Quantum Dot Cytotoxicity and Cellular Uptake Using Microfluidic System

Jing Wu,<sup>a,b</sup> Haifang Li,\*<sup>a</sup> Qiushui Chen,<sup>a</sup> Xuexia Lin,<sup>a</sup> Wu Liu,<sup>a</sup> and Jin-Ming Lin\*<sup>a</sup>*Received (in XXX, XXX) Xth XXXXXXXXXX 20XX, Accepted Xth XXXXXXXXXX 20XX*

DOI: 10.1039/b000000x

This paper reports a novel method for statistic analysis of quantum dot (QD) cytotoxicity and cellular uptake basing on single cell cycles, which is a series works of the study of QD cytotoxicity using microfluidic system (*Lab Chip*, 2012, **12**, 3474-3480; 2013, **13**, 1948-1954). The specially designed microfluidic system consisted of polydimethylsiloxane (PDMS) microwell array for single-cell arrangement and microchannels for QD solution diffusion, enabling effectively controlling stable cell density and interdistance between them, as well as maintaining a constant QD concentration with disturbance-free of fluids to cellular uptake. We showed that the treatments of QDs had no influence on cell cycles. However, the QD cytotoxicity was found to be dependent on cellular uptake in various cell cycle phases, because the accumulation and dilution of QDs happened in single cell cycles. The rank of QD cytotoxicity was G2/M > S > G0/G1. Thus, this technology could be served as a new strategy to investigate otherwise inaccessible mechanisms governing nanoparticle cytotoxicity.

## Introduction

Nanomedicine is increasingly emerging as a tremendously promise strategy for the therapy and imaging of major disease using nanoparticles (NPs). Of great interest, quantum dots (QDs) have been extensively utilized in cellular imaging and drug delivery owing to their outstanding fluorescent properties<sup>1-3</sup> and tiny size.<sup>4-6</sup> However, cytotoxicity of QDs becomes a major obstacle to universal application of nanomedicine, thus attracts particular attentions in current years.<sup>7-10</sup>

Recently, cellular uptake of NPs was reported to be influenced by cell cycle<sup>11</sup> and cell-to-cell interaction.<sup>12</sup> Cellular uptake of NPs also depended on the properties of cellular protein corona-NPs complexes.<sup>13-15</sup> On the other hand, the cellular microenvironment, such as cell-to-cell distance and NPs fluid conditions, might also affect the cellular uptake. Typically, the cytotoxicity of QDs is commonly studied by an average result from cell populations,<sup>16-18</sup> thus challenging to deeply understand the complex mechanisms of QD cytotoxicity. For these reasons, the statistic analysis of cellular uptake base on single cell cycles will be particularly acute in the investigation of QD cytotoxicity under a precisely defined microenvironment. Recently, integrated microfluidic technology is considered as a powerful tool for spatially and temporally controlling cell growth and stimuli, as well as providing unique advantages of long term cell culture and high-throughput analysis.<sup>19-22</sup> For example, a serie of cell densities could be generated<sup>23</sup> and cells could be precisely paired to study cell fusion on the microfluidic chip.<sup>24</sup> Microfabricated device also worked as a platform that providing novel means for probing single-cell behavior without flow-induced shear stress.<sup>25</sup> To our knowledge, the statistic assays of QD cytotoxicity by

considering single cell cycles on a well-defined platform will show great significance.

Here, we developed a microfluidic cell-culture system to exploit the statistic analysis of QD cytotoxicity and cellular uptake based on single cell cycles. The design of polydimethylsiloxane (PDMS) microwell array for single-cell arrangements allowed effectively controlling stable cell density and how close they were, which was critical to statistic analysis of cellular uptake. Besides that, microfluidic structure was specially designed for the QD solution diffusing from the side channels to the central one, enabling to maintain a constant QD concentration and avoid the influences of fluids on cellular uptake. This novel technique for well-defined cellular microenvironments was considered as a powerful strategy to construct a stable and controllable platform for QD cytotoxicity assays based on single cell cycles.

## Experimental Section

### Fabrication of microfluidic device

Standard soft lithography and replica molding techniques were used to fabricate the PDMS microwell array which was utilized for single cell capture. Briefly, silicon wafer (Tianjin, China) was cleaned by piranha solution beforehand and negative photoresist SU-8 2050 (Microchem, Newton, MA) was spun onto it at the speed of 3000 rpm to assist the micropillar attachment onto the silica wafer. After baking it to be dry, the photoresist coating was put under UV light exposure without any mask. Then, negative photoresist SU-8 2015 was spin-coated onto it at the same speed to control the depth of microwell to be ~20  $\mu\text{m}$ . Re-exposure technology was used to fabricate the different heights of

microchannels on the upper PDMS. Negative photoresist SU-8 2007 was utilized to generate the layer of low microchannels and SU-8 2050 was taken to manufacture the layer of high main channels. Both the two molds were finished through the following steps: UV light exposure, development and silanization. PDMS prepolymer and curing agent (Dow Corning, Sylgard 184, Midland, MI, USA) were premixed as 10:1 (by mass) and poured onto the molds. The mixture was degassed under vacuum for 0.5 h and put into an oven for curing at 75 °C for 2 h. The PDMS was peeled off carefully and cut into the designed shape. Inlets and outlets of microchannels were made by a flat-tipped syringe needle. The two PDMS replicas were sealed together via oxygen plasma (PDC-32 g, Harrick Plasma, Ithaca, NY, USA) treatment for 90 s. The device was sterilized under UV light for 5 min before use.

### Operation of single cell array on the microfluidic device

A confluent 60-mm-diameter petri dish of HepG2 cells (Cancer Institute & Hospital Chinese Academy of Medical Science, Beijing, China) were trypsinized and cell suspension was collected. The suspension was centrifuged and the supernatant was removed. The remained cells were resuspended in 100  $\mu\text{L}$  cell culture medium and infused into the channel 2 which covered on the PDMS microwell array. The microfluidic device had been kept in setting for 3 min to make cells fall into microwells and surplus cells were flushed out by cell culture medium. Single cell capture was observed and analyzed under Leica DMI 4000 B fluorescent microscope (Wetzlar, Germany).

The captured cells were continued to be cultured on the microfluidic device in incubator for 1-3 days. Cell viability was detected by live/dead assay kit (calcein-AM/EthD-1, Invitrogen, CA, USA) to demonstrate nonperturbing of the microfluidic device. Fluorescent images were taken by the same microscope and the data were analyzed by program Image-Pro Plus 6.0.

### Cell cycle assay on flow cytometry

For cell cycle assay, confluent 60-mm-diameter plates of HepG2 cells were divided evenly into four 35-mm-diameter plates and then cultured to be the abundance of 80%. QD solution ( $5 \mu\text{g mL}^{-1}$ ) was added into two petri dishes and the other two ones without any treatment were used as control. After 24 h, all these HepG2 cells were harvested by 0.05% trypsin-ethylenediaminetetraacetic acid and cell cycle were studied by total DNA staining on flow cytometry. Cells were fixed with 70% ice-cold ethanol for 1 h at 4 °C and centrifugated. The collected cells were rinsed with phosphate buffer saline (PBS) and resuspended in 500  $\mu\text{L}$  PBS containing 50  $\mu\text{g mL}^{-1}$  propidium iodide (PI), 50  $\mu\text{g mL}^{-1}$  RNase A and 3.8 mM sodium citrate for 30 min incubation.

### Cell cycle and QD cytotoxicity

After cultured on the microfluidic device for 1 day, the captured cells were treated by QDs for 24 h under static and dynamic conditions, respectively. Stocking solution of QDs ( $5 \text{ mg mL}^{-1}$ ) was serially diluted by cell culture medium into the desired concentration ( $5 \mu\text{g mL}^{-1}$ ) and infused into the channel 1. Cell culture medium as the blank solution was infused into the channel 3. The two kinds of solutions diffused into the channel 2 through the low microchannels under static condition. For dynamic condition, QD solution ( $5 \mu\text{g mL}^{-1}$ ) and cell culture medium were

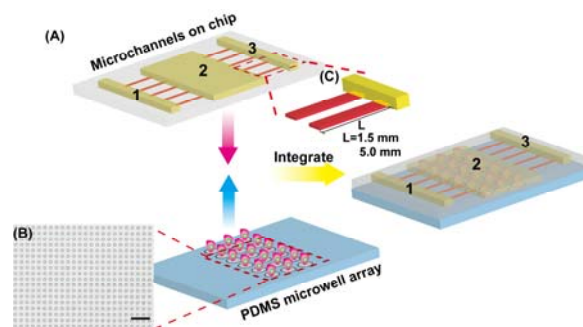


**Fig. 1.** Schematic illustration of microfluidic device for the statistic analysis of QD cytotoxicity based on single cell cycle observation. (A) The two functional components: PDMS microwell array and microchannels on the chip. The microfluidic device is the integration of them. (B) The microscope image of the PDMS microwell array (Scale bar: 250  $\mu\text{m}$ ). (C) Schematic representation of the microchannels with different heights on the chip. The length of lower microchannel was designed to be 1.5 mm and 5.0 mm, respectively.

injected into the channel 1 and 3 respectively at the speed of 0.6  $\mu\text{L min}^{-1}$  using syringe pump (Harvard Apparatus PHD 2000, Holliston, MA). Intracellular reactive oxygen species (ROS) and glutathione (GSH) were detected as two indexes of QD cytotoxicity. 10  $\mu\text{M}$  Hoechst 33342 (Invitrogen, CA, USA) and 100  $\mu\text{M}$  dihydroethidium (DHE) (Beijing, China) were used to stain cells simultaneously for ROS analysis in different cell cycle phases. Fluorescent images were taken twice at the same position under two different exciting wavelengths ( $\lambda_{\text{ex}} = 340\text{-}380 \text{ nm}$  and  $\lambda_{\text{ex}} = 535 \text{ nm}$ ) with a fluorescence microscope equipped with a cooled CCD camera with software of Leica Application Suite, LAS V2.7. Intracellular GSH variation of cells in different cycles also was detected by the similar method but the difference was that cells were stained by Hoechst 33342 and 2,3-naphthalenedicarboxaldehyde (NDA) (Tokyo, Japan) at the same time. Cell cycle was analyzed by software Origin, and program QCapture Pro (Version 5.1.1.14, Media Cybernetics, USA) was utilized to analyze fluorescent intensity of intracellular ROS and GSH.

## Results and Discussion

### Design of the microfluidic device

The microfluidic device was fabricated by re-exposure technology and multi-layer soft lithography. The designed microdevice consisted of two functional components (Figure 1A): 1) a PDMS microwell array substrate for capturing single cells with controllable cell density and interdistance between them, and 2) an overlaid PDMS microchannels with different heights for maintaining stable QD concentration and culturing single cells without shear stress. The diameter and depth of microwells were designed to be 25  $\mu\text{m}$  and 20  $\mu\text{m}$  (Figure 1B), respectively, which were suitable to capture HepG2 cells. The microchannels on the top layer included two parts: three main channels and the connecting microchannels. The QD solution and cell culture medium could diffuse from the channel 1 and 3 into the channel 2 through the lower connecting microchannels (Figure 1C). There are two different lengths (1.5 mm and 5.0 mm) of the low microchannels to illuminate the impacts of diffusion distance and concentration-dependent of QD cytotoxicity. The solution

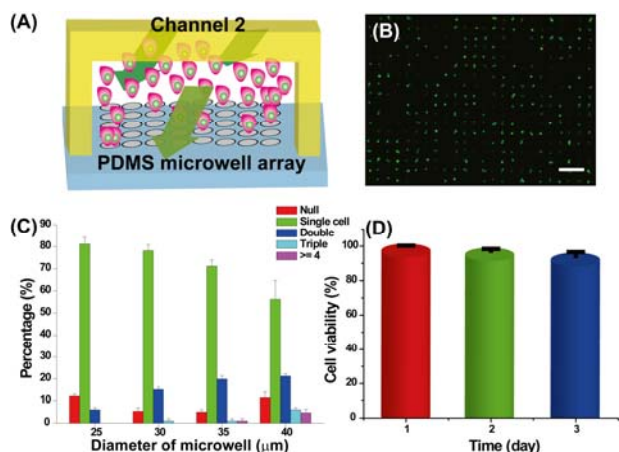


**Fig. 2.** Single cell array on the microfluidic device. (A) Schematic representation of the operation process for generating single cell array. (B) Fluorescent images of single cell array (Scale bar: 200 μm). (C) Cell distribution in different size of PDMS microwell array. (D) Cell viability detection on the microfluidic device during 1-3 days.

concentration in the channel 2 tended to be stable after a few hours diffusion, forming a dilute-free condition. It was very critical to eliminate the effect of fluid on cellular uptake and the generated shear stress.

### Single cell array on the microfluidic device

Single-cell array is particularly useful to study cellular heterogeneity.<sup>27, 28</sup> The depth of microwells was controlled to be 20 μm which was comparable to the diameter of HepG2 cells (~16 μm). More than one cell would be contained in the deeper microwells while cells in the shallow ones could not be confined in them during the operation process. The interdistance between the cells could be regulated through controlling the interwell distance, which was 50 μm in this case. During loading, cells were filled into the channel 2 and passed through the microwell array (Figure 2A). Actually, different microwell diameters of 25, 30, 35 and 40 μm were tested in this system. For the microwell with a diameter of 25 μm, the overall cell occupancy was approximately 90% and almost all the occupied microwells included only one cell (Figure 2B and 2C). The microwells with diameters of 30 and 35 μm have higher overall cell occupancy while the microwells with two to four cells also increased significantly. Cells conveniently entered into larger microwells but they also were easily to be flushed out, so the number of null microwells added leading to a low cell occupancy for microwell diameter of 40 μm (Figure 2C and S1). As a result, size of microwell of 25/20 μm (diameter/depth) was selected to conduct the statistic analysis of QD cytotoxicity finally. The microwell array was 20×150 and the volume of channel 2 was 6 μL. Loading efficiency was about 80% making sure that the cell concentration in channel 2 reached as high as ~10<sup>8</sup> mL<sup>-1</sup> and was satisfied with the request of this study. The concentration of single cells could be regulated through designing the number of microwells and the size of channel 2.

The captured single cells were further cultured in the microwells. Cell viability was detected by live/dead (calcein AM/EthD-1) assay kit. The results indicated that the viability of HepG2 cells kept above 90% during the 1-3 days (Figure 2D) and

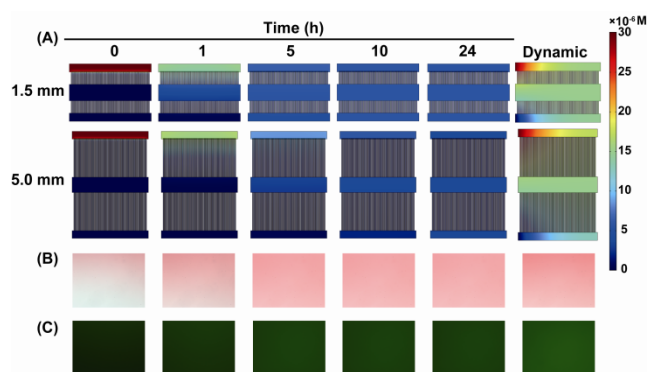


**Fig. 3.** Concentration of solutions in the microchannels keeps constant under static and dynamic conditions, respectively. (A) Concentration simulation by Software COMSOL Multiphysics. Amaranth (B) and fluorescein sodium (C) solutions diffuse in the channel 2 observing by microscope.

demonstrated that the operation of generating single cell array and the microwells bring no adverse impact on cell viability. A nonperturbing single cell array generation mechanism was provided and the interdistance and concentration of the single cells were controllable on this microfluidic device.

### Simulation of QD concentration in the microchannels

To protect cells from shear stress effect, solutions were controlled to diffuse from the side channels into the middle channel which covered on the single cell array. Software COMSOL Multiphysics was used to simulate the process under static and dynamic conditions respectively (Figure 3A and Figure S2). The low microchannels were designed to be 1.5 mm and 5.0 mm long to make know how diffusion distance affected on QD cytotoxicity. Concentration in channel 2 reached balance after a few hours under static condition both on the two kinds of microfluidic devices. It is worthwhile to point out that the time taking to reach balance is different: 5 h for the 1.5 mm-microfluidic device while as long as 10 h on the 5.0 mm-microfluidic device. Comparing to the long microchannels, the concentration is higher in the short ones at the same time point. Data in Supporting Information Figure S2 also shows this tendency. At the dynamic condition, the concentration in channel 2 has no obvious variation all through the 24 h which is higher than that of static condition. Amaranth and fluorescein sodium (100 μM) solutions were used to observe the diffusion process. The microscope images were accordance with the simulated results (Figure 3B and 3C). The results indicate that the concentration of solutions in channel 2 could keep invariable both under static and dynamic conditions. All the single cells were cultured in a fluid disturbance- and shear stress-free microenvironment.

### The effect of QD cytotoxicity on cell cycle

In order to analyze the impact of QDs on cell cycle distribution, DNA staining with PI was analyzed on flow cytometer. The fluorescent intensity of PI was proportional to the quantity of intracellular DNA, according to which cell cycle was divided to be G0/G1, S and G2/M phases. For cells treated by QDs, the population distributed in G0/G1, S and G2/M phases is 64.21%, 22.80% and 12.99%, respectively. The population of cells without any treatment distributed in G0/G1, S and G2/M phases

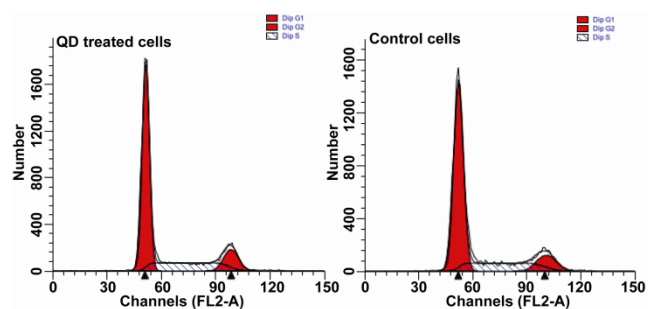


**Fig. 4.** Cell cycle of QDs treated and control cells analysis on flow cytometer.

**Table 1.** The population of cells distributed in different cell cycle phases based on flow cytometer detection.

Cell cycle	QD treated cells	Control cells
G0/G1	64.21%	67.54%
S	22.80%	21.09%
G2/M	12.99%	11.38%

is 67.54%, 21.09% and 11.38% (Figure 4 and Table 1). The population of cells treated by QDs in different phases have no obvious change compare to control cells. The type and concentration of QDs used here do not perturb cell cycle distribution and are suitable for studying the effect of cell cycle on QD cytotoxicity.

#### Role of cell cycle on QD cytotoxicity

The relationship between cell cycle and cytotoxicity of QDs was assayed on the microfluidic platform we constructed. ROS generation and GSH reduction as cellular signal molecules representing redox state were detected as two cytotoxic indexes in this work.<sup>29-31</sup> DHE and NDA were used as two specific fluorescent probes to detect them. Generally, the quantity of intracellular ROS generation keeps at low level and could be easily neutralized by GSH and other antioxidant enzymes. However, QDs are outstanding energy transferors aiding to ROS generation and GSH reduction so the fluorescence of ROS was enhanced while fluorescence of GSH was weakened in the presence of QDs.

Cell cycle was considered to be an important cellular factor in biological process. Cell cycle could be divided into four different phases: G1, S, G2 and M. The main task in G1 phase for cells is synthesizing RNA and ribosome, and cell volume is remarkably increased. Cells in G1 phase prepare nutrition and energy for entering into S phase. DNA is synthesized in S phase and protein is fabricated in G2 phase. After the three phases, cells get into M phase and start division. The two daughter cells restart a new cell cycle by commencing with G1 phase. To identify the cell cycle, Hoechst 33342 and DHE or NDA were simultaneously stained the cells and fluorescent images were taken at the same conditions by the fluorescent microscope. Hoechst 33342 is a fluorescent probe that specific to nucleus acid staining so the integrated intensity of the same area on fluorescent images was proportional to the quantity of nucleic acid which was relative to cell cycle phases. The nucleic acid of cells in different phases is various in quantity: G0/G1 phase is 2N, G2/M phase is 4N and S phase falls in between. It is reasonable to refer that the highest

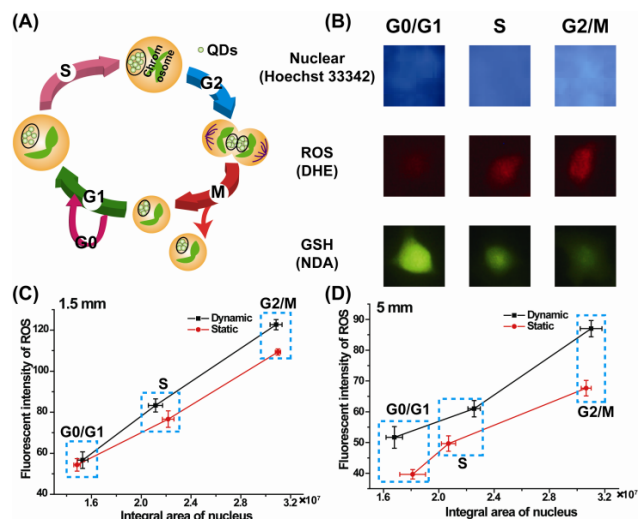


**Fig. 5.** Single cells in different cell cycle phases response to QD cytotoxicity. (A) Schematic representation of QD uptake of cells in different cell cycle phases. (B) Fluorescent images of ROS and GSH in different cell cycle phases which were characterized by two fluorescent probes simultaneous staining. (C) Curves of fluorescence of ROS variation in different cell cycle phases under dynamic and static conditions on 1.5 mm-microfluidic device. (D) Curves of fluorescence of ROS variation in different cell cycle phases under dynamic and static conditions on 5.0 mm-microfluidic device.

integrated intensity was assigned to the cell in G2/M phase while the lowest one was noted the cell in G0/G1 phase and the integrated intensity of the cell in S phase is middle. As a result, two specific fluorescent probes simultaneously stain cells could identify the degree of cytotoxicity of the single cells in different cell cycle phases and make know the relationship between cell cycle and QD cytotoxicity.

Fluorescent images in Figure 5B demonstrated that the fluorescence of nucleic acid ranged in the rank G2/M > S > G0/G1 and the fluorescence of ROS varied as the same sequence. Redundant ROS reacted with intracellular GSH so the rank of fluorescent intensity of GSH of cells in different cell cycle phases arranged in the opposite order (Figure 5B and 6). As shown in Figure 5C and 5D, curves of fluorescent intensity variation of cellular ROS in different cell cycle phases exhibited the above tendency both on the two kinds of microfluidic device. Various cellular uptake of QDs in different cell cycle phases<sup>11</sup> is explained as the main reason responsible for the differentiation of QD cytotoxicity. Rise of membrane tension of metaphase cells leading to dramatic inhibition of endocytosis. Morphology of cells also changes during cell cycles, while total membrane area and surface expression of membrane-bound proteins vary during cell division.<sup>32</sup> Possibly, cell cycle gives a certain impact on cellular uptake for series of events happen during the four phases.<sup>32-34</sup> QDs is internalized through autophagy and remained in lysosomes.<sup>13</sup> Uptake rates in different cell cycle phases are similar and cell export is negligible once the QDs were internalized.<sup>11</sup> However, uptake time for cells in different cell cycle phases is not the same. Cells in G2/M phase have the longest uptake time for that they have not divided and intracellular QDs have not been diluted into the cells of next generation. Cells in G0/G1 phase have the shortest uptake time for they just have finished division and almost have no time to

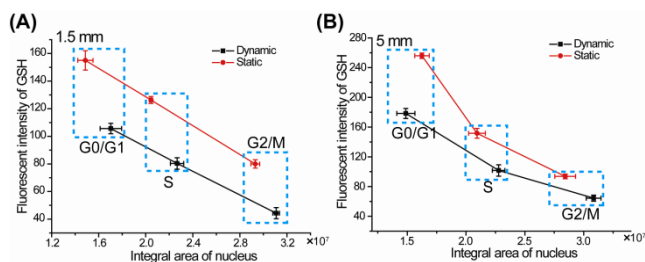


**Fig. 6.** Fluorescent intensity of intracellular GSH variation on the two kinds of microfluidic device. (A) Curves of fluorescence of GSH variation in different cell cycle phases under dynamic and static conditions on 1.5 mm-microfluidic device. (B) Curves of fluorescence of GSH variation in different cell cycle phases under dynamic and static conditions on 5.0 mm-microfluidic device.

accumulate more QDs. The uptake time of cells in S phase ranks between the above two phases and cells have internalized some QDs after cell division. As a result, the QD accumulation in cells of different phases rank in the sequence that  $G2/M > S > G0/G1$  (Figure 5A) then the different intracellular QD concentrations lead to various cytotoxic effect. Two different lengths of low microchannels (1.5 mm and 5.0 mm) were designed and the rule was reproved both on the two kinds of microfluidic device (Figure 5C, 5D and 6).

In addition to the differentiation of cell cycle phases, the comparison between the dynamic and static conditions also show that it is observed more severe cytotoxicity of QDs under dynamic condition at the same cell cycle phases. The results could be explained that the QDs concentration in channel 2 keeps higher under dynamic condition. The concentration difference between the two different long microchannels (Figure 3A) also bring the same effect, the fluorescent intensity of ROS is higher on the 1.5 mm-microfluidic chip while the fluorescent intensity of GSH is lower (Figure 5C, 5D and 6). The diffusion distance plays a certain role in QD cytotoxicity, which is accordance with the reported results.<sup>35</sup>

## Conclusions

In summary, a microfluidic device for single cell cycle observation was developed and the affect of cell cycle phases on QD cytotoxicity was demonstrated on this platform. QD accumulation in different phases ranked in the order  $G2/M > S > G0/G1$  leading to QD cytotoxicity of cells in various phases also ranged in the same order. The results implicated that cell cycle phases also was a considerable factor during the biological or toxicological study. Cell cycle must be accommodated in the future studies and models helping to understand the mechanism of QD cytotoxicity. It is noted that cancerous cells experience the S or G2/M phases more often than normal cells for they divide faster so the dilution of QDs is greater. The results implicate that the imaging or therapy targeting of cancerous cells using QDs is suggested to take combined strategies in which one component slows or arrests cell division and another one implement the imaging or therapy. Comparison between dynamic and static conditions and different diffusion distances also were conducted and the results were well agreed with previous report. The multi-functional microfluidic device is easily to be fabricated and potentially be attached into high-throughput analysis systems for single cell researches.

## Acknowledgments

This work was supported by the National Natural Science Foundation of China (Nos. 91213305, 20935002, 21275088) and China Equipment and Education Resources System (No. CERS-1-75).

## Notes and references

- <sup>a</sup> Department of Chemistry, Beijing Key Laboratory of Microanalytical Methods and Instrumentation, Tsinghua University, Beijing 100084, China. Tel/Fax: (+86) 10 62792343; E-mail: jmlin@mail.tsinghua.edu.cn.
- <sup>b</sup> School of Science, China University of Geosciences (Beijing), Beijing 100083, China.
- \*Corresponding authors. jmlin@mail.tsinghua.edu.cn (Prof. Jin-Ming Lin), lihaifang@mail.tsinghua.edu.cn (Dr. Haifang Li)
- † Electronic Supplementary Information (ESI) available: single cell capture on the microfluidic device, concentration of QD solution simulation in the microchannels and QD cytotoxicity detection by CCK-8 assay kit. See DOI: 10.1039/b000000x/
1. E. Pösel, C. Schmidtke, S. Fischer, K. Peldschus, J. Salamon, H. Kloust, H. Tran, A. Pietsch, M. Heine, G. Adam, U. Schumacher, C. Wagener, S. Förster and H. Weller, *ACS Nano*, 2012, **6**, 3346-3355.
  2. X. Wu, H. Liu, J. Liu, K. N. Haley, J. A. Treadway, J. P. Larson, N. Ge, F. Peale and M. P. Bruchez, *Nat Biotechnol*, 2003, **21**, 41-46.
  3. D. R. Larson, W. R. Zipfel, R. M. Williams, S. W. Clark, M. P. Bruchez, F. W. Wise and W. W. Webb, *Science*, 2003, **300**, 1434-1436.
  4. M. Green, *Angew. Chem. Int. Ed.*, 2004, **43**, 4129-4131.
  5. F. Song, P. S. Tang, H. Durst, D. T. Cramb and W. C. Chan, *Angew. Chem. Int. Ed.*, 2012, **51**, 8773-8777.
  6. C. Wu and D. T. Chiu, *Angew. Chem. Int. Ed.*, 2013, **52**, 3086-3109.
  7. W. E. Smith, J. Brownell, C. C. White, Z. Afsharnejad, J. Tsai, X. Hu, S. J. Polyak, X. Gao, T. J. Kavanagh and D. L. Eaton, *ACS Nano*, 2012, **6**, 9475-9484.
  8. N. Chen, Y. He, Y. Su, X. Li, Q. Huang, H. Wang, X. Zhang, R. Tai and C. Fan, *Biomaterials*, 2012, **33**, 1238-1244.
  9. C. Kirchner, T. Liedl, S. Kudera, T. Pellegrino, A. Muñoz Javier, H. E. Gaub, S. Stölzle, N. Fertig and W. J. Parak, *Nano Lett*, 2005, **5**, 331-338.
  10. A. Nel, T. Xia, L. Mädler and N. Li, *Science*, 2006, **311**, 622-627.
  11. J. A. Kim, C. Aberg, A. Salvati and K. A. Dawson, *Nat. Nanotechnol.*, 2012, **7**, 62-68.
  12. B. Snijder, R. Sacher, P. Ramo, E. Damm, P. Liberali and L. Pelkmans, *Nature*, 2009, **461**, 520-523.
  13. A. Lesniak, A. Campbell, M. P. Monopoli, I. Lynch, A. Salvati and K. A. Dawson, *Biomaterials*, 2010, **31**, 9511-9518.
  14. A. Lesniak, A. Salvati, M. J. Santos-Martinez, M. W. Radomski, K. A. Dawson and C. Aberg, *J. Am. Chem. Soc.*, 2013, **135**, 1438-1444.
  15. M. P. Monopoli, C. Aberg, A. Salvati and K. A. Dawson, *Nat. Nanotechnol.*, 2012, **7**, 779-786.
  16. A. Nagy, J. A. Hollingsworth, B. Hu, A. Steinbruck, P. C. Stark, V. C. Rios, M. Vuyisich, M. H. Stewart, D. H. Atha, B. C. Nelson and R. Iyer, *ACS Nano*, 2013, **7**, 8397-8411.
  17. Y. Li, Y. Zhou, H. Wang, S. Perrett, Y. Zhao, Z. Tang and G. Nie, *Angew. Chem. Int. Ed.*, 2011, **50**, 5860-5864.
  18. K. C. Nguyen, W. G. Willmore and A. F. Tayabali, *Toxicology*, 2013, **306**, 114-123.
  19. D. Huh, B. D. Matthews, A. Mammoto, M. Montoya-Zavala, H. Y. Hsin and D. E. Ingber, *Science*, 2010, **328**, 1662-1668.
  20. J. El-Ali, P. K. Sorger and K. F. Jensen, *Nature*, 2006, **442**, 403-411.
  21. V. Lecault, M. VanInsberghe, S. Sekulovic, D. J. H. F. Knapp, S. Wohrer, W. Bowden, F. Viel, T. McLaughlin, D. Falconnet and A. K. White, *Nat. Methods*, 2011, **8**, 581-586.
  22. P. Neuzi, S. Giselbrecht, K. Lange, T. J. Huang and A. Manz, *Nat Rev Drug Discov*, 2012, **11**, 620-632.
  23. J. Wu, Q. Chen, W. Liu and J.-M. Lin, *Lab Chip*, 2013, **13**, 1948-1954.
  24. A. M. Skelley, O. Kirak, H. Suh, R. Jaenisch and J. Voldman, *Nat. Methods*, 2009, **6**, 147-152.

- 
25. M. Kolnik, L. S. Tsimring and J. Hasty, *Lab Chip*, 2012, **12**, 4732-4737.
26. M. Morel, J. C. Galas, M. Dahan and V. Studer, *Lab Chip*, 2012, **12**, 1340-1346.
- 5 27. D. Bakstad, A. Adamson, D. G. Spiller and M. R. White, *Curr Opin Biotechnol*, 2012, **23**, 103-109.
28. D. G. Spiller, C. D. Wood, D. A. Rand and M. R. H. White, *Nature*, 2010, **465**, 736-745.
29. B. R. Singh, B. N. Singh, W. Khan, H. B. Singh and A. H. Naqvi,  
10 *Biomaterials*, 2012, **33**, 5753-5767.
30. A. Nel, *Science*, 2005, **308**, 804-806.
31. A. S. Thakor, R. Paulmurugan, P. Kempen, C. Zavaleta, R. Sinclair,  
T. F. Massoud and S. S. Gambhir, *Small*, 2011, **7**, 126-136.
32. E. Boucrot and T. Kirchhausen, *Proc. Natl. Acad. Sci. USA*, 2007,  
15 **104**, 7939-7944.
33. J. K. Schweitzer, E. E. Burke, H. V. Goodson and C. D'Souza-  
Schorey, *J Biol Chem*, 2005, **280**, 41628-41635.
34. D. Raucher and M. P. Sheetz, *J Cell Biol*, 1999, **144**, 497-506.
- 20 35. J. Wu, Q. Chen, W. Liu, Y. Zhang and J.-M. Lin, *Lab Chip*, 2012, **12**,  
3474-3480.